

Investigations on the Effect of Chitin Nanofiber in PMMA Based Solid Polymer Electrolyte Systems

P.M. Shyly¹, S. Dawn Dharma Roy², Paitip Thiravetyan³, S. Thanikaikarasan¹, P.J. Sebastian^{4,†},
D. Eapen⁵ and X. Sahaya Shajan^{1,*}

¹Centre for Scientific and Applied Research, School of Basic Engineering and Sciences,
PSN College of Engineering and Technology, Tirunelveli- 627 152, Tamil Nadu, India

²Department of Physics, Nesamany Memorial Christian College, Marthandam-629 165, Tamil Nadu, India

³School of Bioresources and Technology, King Mongkut's University of Technology Thonburi, Bangkok 10150, Thailand

⁴Instituto de Energias Renovables-UNAM, 62580, Temixco, Morelos, Mexico

⁵Instituto de Biotecnología-UNAM, Av. Universidad 2001, Cuernavaca, Morelos, 62210, Mexico

Received: February 18, 2014, Accepted: July 20, 2014, Available online: October 03, 2014

Abstract: Polymer electrolyte membranes find application in a variety of fields such as battery systems, fuel cells, sensors and other electrochemical devices. In this paper we have done some investigations on the effect of chitin nanofiber (CNF) in PMMA based solid polymer electrolyte systems. CNF was synthesized from shrimp cell chitin by stepwise purification and acid hydrolysis method. PMMA based electrolyte films containing different concentrations of lithium salt and CNFs as filler were prepared by hot-press membrane technique. Crystalline nature and phase changes in polymer electrolytes were confirmed by X-ray diffraction analysis. Thermal behavior of the polymer electrolyte systems was studied by differential scanning calorimetry. Ionic conductivities of the electrolytes have been determined using a.c. impedance analysis in the temperature range between 303 and 393K. The temperature-dependent ionic conductivity plots seemed to obey the VTF relation. Dielectric relaxation studies of the polymer electrolyte have been done and the results are discussed.

Keywords: Chitin nanofiber, polymer electrolytes, fuel cell, PMMA, Dielectric studies

1. INTRODUCTION

During the last three decades, various attempts have been made by a number of researchers for the development of suitable polymer electrolytes. This is because of the reason that they find wide range applications in a variety of electrochemical devices such as batteries, supercapacitors, electro-chromic devices and sensors [1-4]. These types of electronic devices require high ion conducting medium that enables it to function at its best [5]. In lithium batteries (LiBs), polymer electrolytes are well adapted to various geometries and are safe compared to conventional liquid electrolytes. Further, it exhibits several interesting properties like flexibility, transparency, lightweight and feasibility of thin film formation. But, the only criterion in polymer electrolytes that affects the polymer lithium ion battery is its low ionic conductivity at ambient

temperature. Hence, much attention is focused on investigating the polymer electrolytes to enhance the ambient temperature conductivity by blending of polymers, cross-linking and incorporation of ceramic fillers or plasticization [6]. In order to obtain a better polymer electrolyte with good conductivity and appropriate mechanical strength, a suitable nanofiller is embedded into the polymer matrix. The transparent polymeric material PMMA possesses many desirable properties such as light-weight, high light transmittance, chemical resistance, uncolored, resistance to weathering corrosion and good insulating properties [7]. PMMA has been used as a polymer host due to its high stability at the lithium-electrolyte interface and also it is less reactive towards the lithium electrode. Moreover, MMA (methyl methacrylate) monomer in PMMA has a polar functional group in the main polymer chain that has a high affinity for lithium ions, which are transported. Oxygen atoms from the MMA structure will form a coordination bond with the

To whom correspondence should be addressed:
Email: *shajan89@gmail.com, †sjp@ier.unam.mx

lithium ion from doping salts. Hence the increase in effective ionic transport of PMMA based polymer electrolytes may be due to the presence of polar functional group in PMMA.

In the present work, chitin nanofiber (CNF) is employed as nanofiller. The natural linear amino polysaccharide chitin (N-acetyl- β -D-glucosamine) possesses several interesting properties such as biocompatibility, bioactive, antimicrobial activity, low toxicity and ecological friendliness. It finds applications in drug delivery system, paper finishing, solid state batteries, food industries and tissue engineering [8]. Lithium triflate (LiCF_3SO_3) is an appealing salt, since it decreases the polymer host's crystallinity and is more thermally and chemically stable than other traditional lithium salts [9].

2. MATERIALS AND METHODS

2.1. Materials

Poly (methyl methacrylate) with an average $M_w = 35,0000$ was obtained from Sigma-Aldrich. Lithium triflate (LiCF_3SO_3) was obtained from Merck and dried at 100°C for 1 hour to eliminate trace amounts of water in the material, prior to the preparation of composite polymer electrolytes. Chitin nanofiber (CNF) was synthesized from shrimp cell according to the method reported earlier [10]. THF obtained from Merck was used as common solvent without further distillation.

2.2. Preparation of Polymer Composite Membrane

The appropriate weight contents of PMMA, CNF and LiCF_3SO_3 were dissolved in tetrahydrofuran (THF). The solution was then stirred continuously until the mixture took a homogeneous viscous liquid appearance. The resulting solution was poured into a Teflon pushes and the THF was allowed to evaporate in air at room temperature. Then the samples were hot pressed into film specimens at high temperature. The thickness of the film was measured by means of a micrometer screw gauge. Different specimens of composite membranes were prepared by varying the amount of polymer and filler. Various compositions of filler, lithium salt and polymer are tabulated in table 1. The homogeneous, self-standing polymer electrolyte films obtained from hot-press method were stored in vacuum desiccators and then subjected to further characterizations.

2.3. Characterization Techniques

2.3.1. XRD Analysis

X-ray diffraction technique is a powerful tool for the study of structural properties of nanomaterials. In the present study, x-ray diffraction measurements have been carried out with $\text{Cu-K}\alpha$ radiation ($\lambda=1.542 \text{ \AA}$). The observed data from XRD spectra have been identified by comparing the recorded patterns with those of the JCPDS-ICDD data files.

Table 1. Compositions of PMMA, Litriplate (LiCF_3SO_3) and CNF

Samples	PMMA (Wt %)	Litriplate (LiCF_3SO_3) (Wt %)	CNF (Wt %)
C0	100	----	----
C1	95	5	----
C2	90	5	5
C3	85	5	10
C4	80	5	15

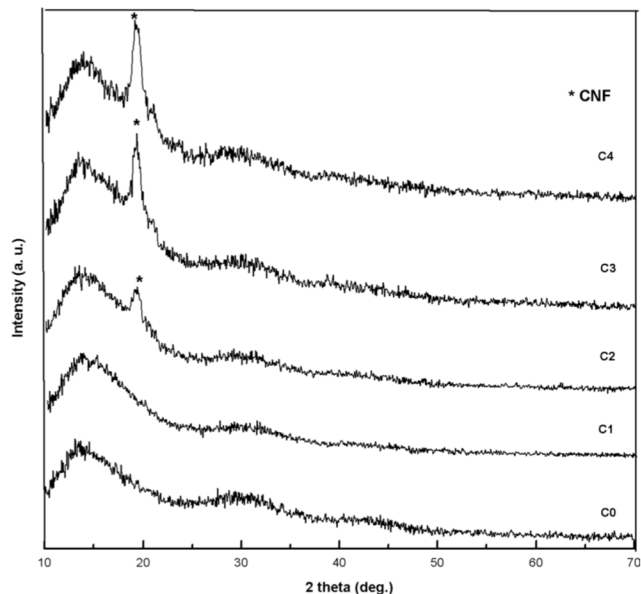


Figure 1. The XRD patterns of: (C0) Pure PMMA, C1, C2, C3, and C4.

2.3.2. Scanning Electron Microscopy

The specimens for the SEM images of the cross-section of the films were prepared by fracturing the films in liquid nitrogen. Scanning electron micrographs of the polymer films were analyzed using SEM.

2.3.3. DSC Analysis

Thermal behavior of mixtures of the polymer, salt, filler and polymer electrolytes were studied by using a differential scanning calorimetry (DSC Q20 V24.2 Build 107). Each sample was scanned from 0 to 250°C with a heating rate of $12.5^\circ\text{C}/\text{min}$ under nitrogen atmosphere. Electrochemical impedance, dielectric and modulus spectroscopic analyses of the membranes were carried out by using electrochemical impedance analyzer (Zahner IM6, Germany) connected to a computer for data acquisition in the frequency range between 75 mHz and 100 kHz . The polymer membranes were kept in a gold plated solid sample holder mounted inside a vacuum cylindrical glass container with signal amplitude of 1V at 16 points per frequency decade from room temperature to 393 K over wide frequency range from 75 mHz to 100 kHz .

3. RESULTS AND DISCUSSION

3.1. XRD Analysis

The x-ray diffraction pattern indicates the amorphous nature with large diffraction maxima that decreases at large diffraction angles. The shape of the first main maximum indicates the ordered packing of the polymer chains. The intensity and shape of the second maxima are related to the effect of ordering inside the main chains. The shape of XRD analysis has been performed and their respective diffraction patterns of pure PMMA, different ratios of PMMA- Li triflate - CNFs based complexes are shown in fig.1 (C0 to C4). The observed broad humps in the XRD spectrum indicate the presence of crystallites of very low dimensions. The symbol * indicates the

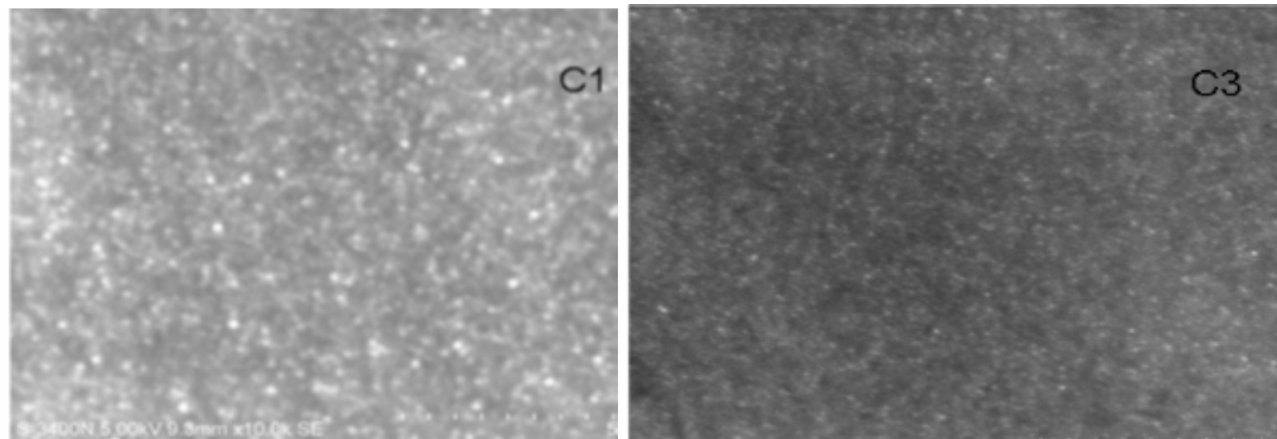


Figure 2. The SEM images of polymer electrolyte C1 (PMMA/ Litriplate) and C4 (PMMA/ Litriplate/ CNF)

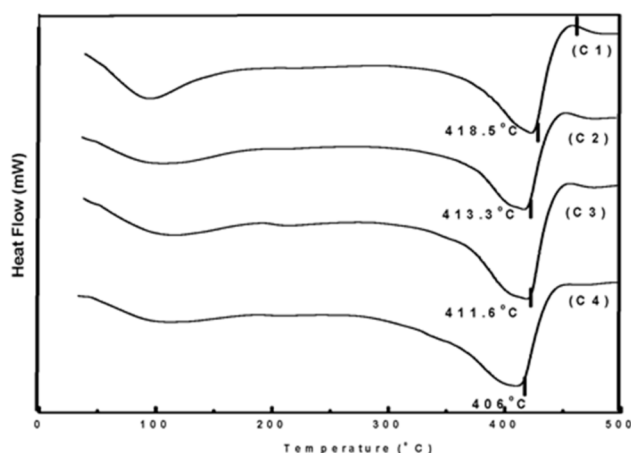


Figure 3. The DSC thermograms of pure PMMA (C0), C1, C3 and C4

diffraction lines from the crystal planes of the CNF specimen which are in agreement with the JCPDS-ICDD 2003 (File No.35-1974) data. The reflections at 2θ value of 19.29 correspond to the crystal planes, viz., (110) yielding the strongest lines as evidenced by the JCPDS file. Peaks corresponding to Li triflate are not observed in the electrolyte leading to the conclusion that Li triflate is dissolved in the polymer matrix and does not remain as a separate phase. There was an increase in relative intensity of the apparent peaks with increasing the filler concentration up to 10%. At $2\theta \approx 19.2^\circ$ there are no peaks in the pure PMMA and C1. As the concentration of CNFs increases the relative intensity also increases and it is slightly shifted towards the right. All the membranes exhibit a broad peak at around $2\theta \approx 14^\circ$ indicating the amorphous structure. The reasons for the absence of sharp peaks may be due to smaller sizes of the particles.

3.2. Scanning Electron Microscopy Analysis

The morphology of the electrolyte film with filler (C1), without filler (C3) was examined by SEM as shown in fig.2. Scanning elec-

tron microscopy images of C1 and C3 electrolytes reveal small difference in surface morphology. Since, both polymer and the fillers are amorphous in nature, there are no crystalline domains but spherulitic structure is evident. C1 and C3 electrolytes show homogeneous, amorphous surface morphology and also possess high interfacial area. Addition of filler resulted in improved surface morphology when compared to polymer-salt complex. The nanoparticles were dispersed well within the remains of the polymer matrix and show no sign of extensive particle agglomeration even after thermal treatment and thereby better connectivity through the polymer that gives rise to high ionic conductivity.

3.3. Differential Scanning Calorimetry Analysis

Thermal studies of the solid polymer electrolyte and its nanocomposite were performed using differential scanning calorimetry. Thermograms of pure PMMA (C0), C1, C2 and C3 are shown in fig.3. Only one T_g appears for all the samples indicating the homogenous nature of the samples [11]. Figure 3 shows the melting temperature of C1, C2, C3 and C4. The incorporation of CNF in the polymer matrix was found to decrease the melting temperature of PMMA as shown in Figure 3. The reduction of the melting peak (T_m) in CNF incorporated membrane may be due to the enhancement of polymer segmental motion as well as increase in amorphous nature induced by the filler-polymer interaction of polymer electrolyte. Hence, the movement of ions in the polymer matrix is increased resulting in the increase of conductivity. This was supported by the observation made in the ionic conductivity studies. The polymeric chain in the amorphous phase is more flexible and provides better segmental motion of the polymer. The reduction of T_m suggested that the interaction between the polymer host backbone and CNF affects the main chain dynamics of the polymer. This is due to the coordination bonds between ether units of PMMA and CNF. The shift towards higher temperature is due to the Li^+ preferring to interact with electron-rich coordinating groups, such as $-O-$ and carbonyl group via transient cross-linkage bonds. These cross-linkage bonds obstruct the rotation of polymer segments and hence increase the energy barrier to the segmental movement. Eventually, this Li^+-O^- binding reduces the flexibility of polymer backbone [12].

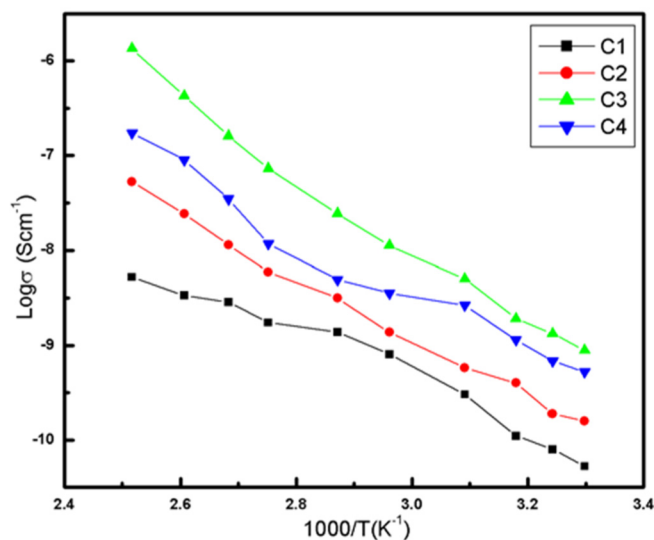


Figure 4. The Arrhenius plots of log of ionic conductivity as a function of reciprocal of temperature for various polymer electrolytes.

3.4. Ionic Conductivity

Ionic conduction in polymer electrolytes may be due to the migration of lithium ions in the free volume of polymer matrix. Variation of ionic conductivity as a function of reciprocal of temperature for polymer electrolytes containing different weight contents of filler and polymer are shown in fig.4. The ionic conductivity of the CNF incorporated polymer electrolytes are determined by means of the following expression,

$$\sigma = \frac{t}{R_b A} \quad (1)$$

where, t and A are the thickness and cross sectional area of the polymer electrolytes. R_b represents the bulk resistance, which is obtained from extrapolation of the semicircular region to high frequencies. It is observed from fig.4 that the conductivity of the polymer electrolyte increases with increase in temperature. i.e., it obeys the Vogel-Tamman-Fulcher (VTF) relation

$$\sigma = AT^{1/2} e^{-B/T_g} \quad (2)$$

where, T_g is the temperature at which the segmental mobility of the polymer backbone ceases to exist and is generally the same as the glass transition temperature. A and B are constants. The constants A in the VTF relation is related to the number of charge carriers and B is related to the activation energy of the ion transport associated with configurational entropy of the polymer electrolyte [13]. It is also noticed from the figure that the conductivity increases with increase in CNF content up to 10 wt%. This may be due to the fact that the CNF increases the polymer chain segmental motion as well as the amorphous region. This amorphous region favors the migration of lithium ion in the free volume of polymer matrix. These results are in agreement with the results reported earlier [12].

The conductivity of CNF incorporated PMMA based polymer electrolytes increases by one order of magnitude compared to filler free electrolyte C1. In the mean time, the incorporation of CNF increases beyond 10 wt%, the sudden decrease in ionic conductivity have observed, which is due to phase discontinuities and dilution effect predominated in the polymer matrix. Also, the addition of lithium salt (Litriflate) in the polymer is optimized and the optimized wt% is 5. When the concentration of Li triflate exceeds 5 wt%, the sample with anion $[\text{CF}_3\text{SO}_3]^-$ forms neutral ion pairs with cation, which leads to decrease in the available number of free moving ions (charge carriers) in the polymer matrix. The maximum ionic conductivity is found to be in the range of $1.35 \times 10^{-5.8}$ S/cm for polymer electrolyte C3 (10 wt% CNF).

3.5. Dielectric Spectral Analysis

The amount of charge that can be stored by polymeric material is evaluated by means of dielectric spectral analysis. In order to confirm that the enhancement of ionic conductivity is due to an increase in available number of mobile charge carriers, the dielectric study was performed. The complex permittivity (ϵ^*) or dielectric constant of a system is defined by

$$\epsilon^* = \epsilon' - j\epsilon'' = \epsilon' - j(\sigma / \omega \epsilon_0) \quad (3)$$

where, ϵ' is the real part of dielectric constant, ϵ'' is the imaginary part of dielectric constant of the material, σ is the conductivity, ω is angular frequency and ϵ_0 is the permittivity of the free space. Fig.5a shows the dielectric constant as a function of logarithmic frequency in the temperature range between 303 K and 393 K using CNF as nanofiller for polymer electrolyte C3. The purpose of choosing electrolyte sample C3 is due the fact that it yields maximum conductivity at room temperature. It is observed from the figure that ϵ' value increases sharply at lower frequency region. The increase in ϵ' at lower frequencies may be due to enhancement of charge carrier density in the space charge accumulation region, which is also known as non-Debye type of behavior [14]. Also, at lower frequencies the contribution of charge carriers increases towards the dielectric constant. This results in an increase in equivalent capacitance at the electrolyte interface. In the mean time, ϵ' decreases at higher frequencies due to the high periodic reversal of the applied electric field at the electrolyte-electrode interface so that there is no excess ion diffusion in the direction of the electric field. It is also evident from fig.5a that as the temperature increases the value of dielectric constant also increases. This is because of the reason that the available number of free moving ions/charge carriers increases at high temperature. Fig.5b shows the variation of dielectric loss (ϵ'') as a function of logarithmic frequency for polymer electrolyte C3 at different temperatures. It is observed from the figure that the dielectric loss increases with increase in temperature and decrease in frequency, which may be due to formation of free charges at the electrolyte-electrode interface. At higher frequencies the dielectric loss decreases owing to the reduction of charge carriers at the interface between the electrode and the electrolyte.

3.6. Dielectric Moduli Studies

In the modulus formalism, an electric modulus M^* is defined in terms of the reciprocal of the complex relative permittivity ϵ^* , i.e.,

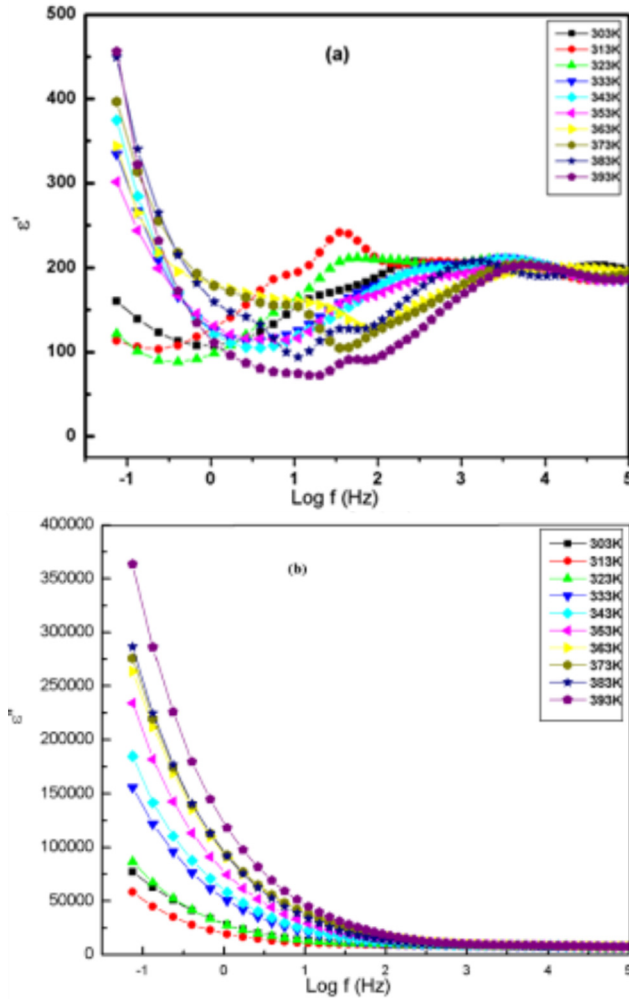


Figure 5. a. The frequency dependence of dielectric constant ϵ' at various temperatures for C3. b. The Frequency dependence of dielectric loss ϵ'' at various temperatures for C3.

$$M^* = \frac{1}{e^*} = M' + iM'' \quad (4)$$

The frequency dependence of M'' at various temperatures for all the samples is shown in fig.6. The maximum of the modulus spectra M'' shifts towards higher frequencies with increase in temperature. The broad nature of the peaks can be interpreted as being the consequence of distributions of relaxation time. Moreover, such peaks are broader than the Debye peak, which is usually attributed to an ideal ionic conductor represented by a single parallel RC element [15]. All the compositions show the same trend. The non-exponential conductivity relaxation can be described by a Kohlrausch-Williams-Watts (KWW) function $\Phi \varphi(t)$, which represents the distribution of relaxation time in ion conducting materials [16]. The electric modulus can be represented as:

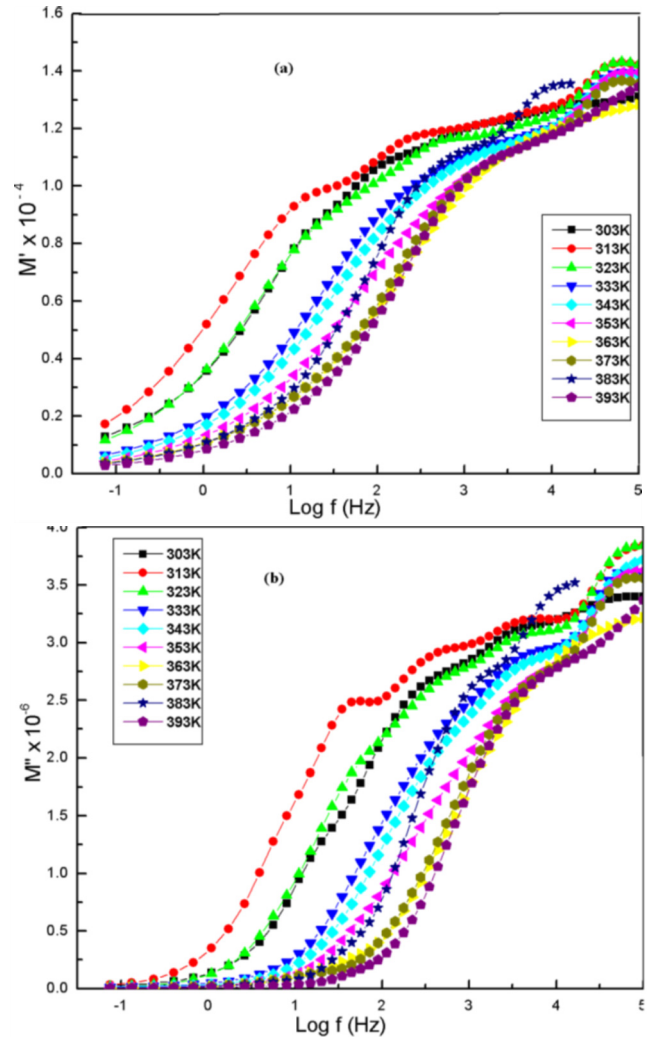


Figure 6. a. The Frequency dependence of the real part of modulus spectra M' at various temperatures for C3. b. The Frequency dependence of the imaginary part of modulus spectra M'' at various temperatures for C3.

$$M^* = M_\infty [1 - \int I dt \exp(-i\omega t) d\phi / dt] \quad (5)$$

$$\varphi(t) = \exp\left[-(t/t_\sigma)^\beta\right] \quad (6)$$

where, $(t_\sigma = 1/2\pi f_p)$ and β are the conductivity relaxation time and the Kohlrausch exponent respectively [17]. The β parameter corresponding to the studied samples was established as a function of temperature using modulus formalism.

Figures 6a, 6b show the frequency dependence of real (M') and imaginary (M'') modulus formalism for sample C3 at different temperatures. At higher frequencies, M' & M'' increase gradually with a tendency for saturation. The observed dispersion is mainly due to conductivity relaxation spread over the range of frequencies. At higher temperatures, the peak shifts to higher frequencies. As the temperature increases, the peaks of M' and M'' have decreased

gradually due to plurality of relaxation mechanism. The value of M' and M'' tends to be zero in the vicinity of lower frequencies which propose that the suppression of the electrode polarization at the interface is negligible at lower frequencies. The presence of long straight line in the low frequency region confirms a large equivalent capacitance associated with the electrode interface. In the mean time, the value of M' and M'' decreased slowly at higher temperature due to decrease in charge carrier density at the space accumulation region. These outcomes are in accordance with the results reported in the literature earlier [18].

4. CONCLUSIONS

SPE consisting of PMMA-Lithium triflate-CNF was prepared and their structural variations were studied. Also, the interaction effect between the fillers and the polymer electrolyte was investigated. SEM and XRD studies confirm the composite nature of the solid polymer electrolyte films. From DSC measurements, an excellent thermal property for the polymer matrix is observed. From DSC analysis, the incorporation of CNF in the polymer matrix was found to decrease the melting temperature of PMMA. Conductivity is found to be depending on both temperature and frequency. At lower frequencies, variations of ϵ' and ϵ'' are shown to be dominated by electrode polarization effect and thus confirming that SPEs of this study are ionic conductors.

REFERENCES

- [1] S. Ahmad, H.B. Bohidar, S. Ahmad, S.A. Agnihotry, *Polymer*, 47, 3583 (2006).
- [2] W. Qiu, X. Ma, Q. Yang, Y. Fu, X. Zong, *J. Power Sources*, 138, 245 (2004).
- [3] S. Ramesh, T. Winie, A.K. Arof, *Eur. Polym. J.*, 43, 1963 (2007).
- [4] A. Manuel Stephan, *Eur. Polym. J.*, 42, 21 (2006).
- [5] A. Manuel Stephan, K.S. Nahm, T. Premkumar, M. Anbukulanthainathan, G. Ravi, J. Wilson, *J. Power Sources*, 159, 1316 (2006).
- [6] S. Ramesh, Liew Chiam Wen, *Ionics*, 16, 255 (2010).
- [7] S. Hirano, ULLMANN's Encyclopedia of Industrial Chemistry, vol. 7, Wiley-VCH, Weinheim, Germany, 6th edition, 2003.
- [8] R.A.A. Muzzarelli, "Chitin chemistry," in *The Polymeric Materials Encyclopedia*, J.C. Salamone, Ed., pp. 312–314, CRC Press, Boca Raton Fla, USA, 1996.
- [9] K.V. Harish Prashanth, R.N. Tharanathan, *Trends in Food Science and Technology*, 18, 117 (2007).
- [10] P.K. Dutta, J. Duta, V.S. Tripathi, *J. of Scientific & Industrial Research*, 63, 20 (2004).
- [11] S. Ramesh, A.K. Arof, *Mater. Sci. Eng., B*, 85, 11 (2001).
- [12] S. Ramesh, A.K. Arof, *J. Power Sources*, 99, 41 (2001).
- [13] P.M. Visakh, Sabu Thomas, *Waste Biomass Valor*, 1, 121 (2010).
- [14] R. Baskaran, S. Selvasekarapandian, N. Kuwata, J. Kawamura, T. Hattori, *Solid State Ionics*, 177, 2679 (2006).
- [15] J. Isasi, M.L. Lopez, M.L. Veiga, E. Ruiz-Hitzky, C. Pico, *J. Solid State Chem.*, 116, 290 (1995).
- [16] G. Williams, D.C. Watts, *Trans. Faraday Soc.*, 66, 80 (1970).
- [17] K.L. Nagi, S.W. Martin, *Phys. Review B*, 40, 10550 (1989).
- [18] A.R. Kulkarni, P. Lunkenheimer, A. Loidl, *Mater. Chem. Phys.*, 63, 93 (2000).